Self-generated Bloch oscillations in biased semiconductor superlattices

Lijun Yang and Marc M. Dignam
Department of Physics, Queen's University, Kingston, Ontario, Canada K7L 3N6
(Received 6 October 2005; revised manuscript received 5 December 2005; published 14 February 2006)

We present theoretical simulations of the highly nonlinear ultrafast intraband response of photoexcited biased semiconductor superlattices. Usually, when Bloch oscillating wave packets are created in superlattices, the required coherences arise purely from a spectrally broad external optical pulse that couples different Wannier-Stark ladder states. However, we show that if the pulse intensity is high enough, then even if the optical pulse is spectrally much narrower than the Wannier-Stark ladder spacing, Bloch oscillating wave packets will be generated by the ultrafast nonadiabatic change in the self-generated internal dc electric field that arises from the formation of excitons with permanent dipole moments.

DOI: 10.1103/PhysRevB.73.075319 PACS number(s): 78.47.+p, 42.65.Re, 73.21.Cd, 78.67.Pt

I. INTRODUCTION

The behavior of electrons in periodic potentials in the presence of external dc and ac electric fields has attracted considerable attention ever since the early days of the quantum treatment of solids. One of the important effects studied in this area was Bloch oscillations (BO's), which involve the dynamic behavior of electrons in a periodic potential in the presence of a uniform, static electric field. BO's were first predicted by Zener[1] in 1934 based on Bloch's work[2] in 1928. In a single-particle picture, the electronic eigenstates of a solid in the presence of an external dc field F_o form the so-called Wannier-Stark ladder (WSL), with the energies given by $E_n=E_0+neF_od$, where d is the lattice period, F_o is the applied dc field, and n is the WSL index.[3–5] BO's occur when wave packets formed from a superposition of these WSL states are generated, for example, by ultrashort optical pulses. The BO frequency is given by $\omega_B \equiv eF_od/\hbar$, which, in the single-particle picture, is only a function of the external dc field F_o.

It took nearly 60 years from the theoretical prediction of the existence of BO's in solids to its experimental confirmation[6–15] in the early 1990s. These experiments and all that followed were performed via the optical injection of carriers into undoped biased semiconductor superlattices (BSSL's). Since then, a series of intensive studies of BO's have been carried out by a number of groups.[9,16–27] In the time domain, BO's were first observed indirectly through four-wave mixing (FWM) experiments[10–13] and then were observed more directly through the emission of terahertz (THz) radiation from Bloch-oscillating carriers in undoped BSSL's.[14,15,22,28]

The above picture of Bloch-oscillating noninteracting electron wave packets is clearly not entirely valid for photoexcited BSSL's. The factors that can modify this picture include interband Zener tunneling,[29] electron-phonon scattering, excitonic effects,[17,18,30,31] and many-body effects. Through miniband engineering, Zener tunneling can be safely neglected for the time periods (a few ps) over which typical experiments are performed. Also, although electron-phonon scattering will eventually destroy the coherences, generally the basic properties of BO's are not affected by this scattering as long as the electron miniband is not appreciably larger than the optical phonon energy (36 meV for GaAs). This scattering simply adds general decoherence and dephasing of the wave packet, which can generally be modeled phenomenologically over the times during which there is still appreciable wave-packet coherence. Excitonic effects have been treated by a number of authors.[30,32–34] We have shown previously[22,23,28,34] that these effects complicate the response significantly, but one can still recognize the basic BO's, which are in fact *excitonic* BO's. Finally, many-body effects encompass a variety of phenomena, including excitation-induced dephasing (EID), hole burning, phase-space filling, and static and dynamic screening.[9,17–21,31,35–43] These effects all play some role in BSSL's. However, as we will see, due to the asymmetry of a BSSL, it is the screening that plays the dominant role.

In this paper, we use an exciton basis and include exciton-exciton interactions to account for static and dynamic screening in the intraband dynamics of photoinjected excitonic wave packets in BSSL's. In a previous publication, we showed that this screening can lead to plasma oscillations (PO's) and the density-dependent frequency of BO's (Ref.

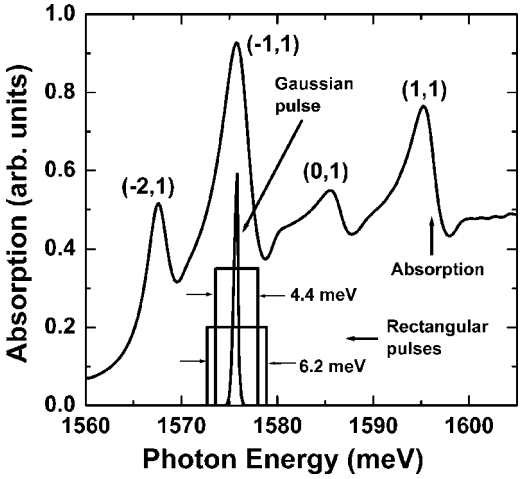

FIG. 1. The calculated linear absorption spectrum for the BSSL with a bias field of $F_o=11.5$ kV/cm. Also shown are the power spectra of the Gaussian optical pulse of Sec. III B and the two spectrally rectangular pulses of Sec. III C.

28) in a BSSL. In this work, we show that, due to this screening, Bloch-oscillating wave packets can be produced via the nonadiabatic change in the total dc bias field arising from the self-generated intraband electric field within the BSSL.

In the standard single-particle picture of BO's, the coherences involved in the coherent Bloch-oscillating wave packets arise purely from the external ultrashort optical pulse and have nothing to do with the many-body interactions among excitons. In other words, the coherences required to produce BO's in a single-particle picture originate from the broad spectral width of the optical pulse, which is wide enough to couple different WSL states. This picture is only valid, however, in the case of low excitation.[22,23] At higher optical intensities, where many-body interactions among excitons have to be taken into account, we find that Bloch-oscillating wave packets arise even if the exciting optical pulse is so spectrally narrow that at low densities it cannot couple different WSL states at all. In this case, the necessary coherences between different WSL states are provided by the nonadiabatic change in the self-induced internal dc electric field in the BSSL; i.e., we obtain *self-generated* BO's (SBO's). We show that these SBO's only arise in theoretical models which treat the dynamics nonperturbatively in the optical field.

The paper is organized as follows. First, in Sec. II, our formalism for treating intraband dynamics nonperturbatively in the optical field is presented. In Sec. III, we present the basic principles of SBO's and how they are generated by spectrally narrow pulses. A comparison between SBO's and PO's is also presented. In Sec. IV, we summarize our results.

II. HAMILTONIAN AND DYNAMIC EQUATIONS

Treating the exciton-exciton interaction in the long-wavelength dipole approximation, the second-quantized Hamiltonian of the BSSL investigated in an exciton basis takes the form[24,27,28]

$$H = \sum_{\mu} \hbar\omega_{\mu} B_{\mu}^{\dagger} B_{\mu} + V\left(- \mathbf{E}_{\text{opt}} \cdot \mathbf{P}_{\text{inter}} + \frac{1}{2\epsilon_0 \epsilon_b} \mathbf{P}_{\text{intra}} \cdot \mathbf{P}_{\text{intra}} \right), \tag{1}$$

where ϵ_0 is the vacuum permittivity, V is the volume of the system, and $B_{\mu}^{\dagger}$ (B_{μ}) is the creation (annihilation) operator for a WSL exciton in the dc field, with internal quantum number μ and energy $\hbar\omega_{\mu}$. The quantity ϵ_b is the dielectric constant, which accounts for the background screening of the Coulomb interaction due to all off-resonant contributions that are not explicitly taken into account.[44] The optical field takes the form

$$\mathbf{E}_{\text{opt}}(t) = \mathcal{E}(t) e^{-i\omega_c t} + \text{c.c.}. \tag{2}$$

where ω_c is the central laser frequency and $\mathcal{E}(t)$ is the ultrafast optical pulse envelope. The polarization operator is defined as

$$\mathbf{P} \equiv \mathbf{P}_{\text{inter}} + \mathbf{P}_{\text{intra}}, \tag{3}$$

where $\mathbf{P}_{\text{inter}}$ and $\mathbf{P}_{\text{intra}}$ denote, respectively, the interband and intraband polarization. The interband polarization is defined as

$$\mathbf{P}_{\text{inter}} \equiv \frac{1}{V} \sum_{\mu} [\mathbf{M}_{\mu} B_{\mu}^{\dagger} + \mathbf{M}_{\mu}^{*} B_{\mu}], \tag{4}$$

where

$$\mathbf{M}_{\mu} = \mathbf{M}_0 \sqrt{A} \int dz \psi^{\mu *}(z,z,0) \tag{5}$$

is the interband dipole matrix element of the μth excitonic state, $|\psi^{\mu}\rangle$. In Eq. (5), $\mathbf{M}_0$ is the bulk interband dipole matrix element and A is the transverse area. The intraband polarization is defined as

$$\mathbf{P}_{\text{intra}} \equiv \frac{1}{V} \sum_{\mu,\mu'} \mathbf{G}_{\mu,\mu'} B_{\mu}^{\dagger} B_{\mu'}, \tag{6}$$

where $\mathbf{G}_{\mu\mu'}$ is the intraband dipole matrix element between two excitonic states $|\psi^{\mu}\rangle$ and $|\psi^{\mu'}\rangle$, given by

$$\mathbf{G}_{\mu\mu'} = \langle \psi^{\mu} | - e(z_e - z_h) | \psi^{\mu'} \rangle. \tag{7}$$

Detailed derivations of these expressions for the polarization are given in our earlier work.[24]

Using the exciton Hamiltonian of Eq. (1) and the Heisenberg equations of motion, we obtain the dynamic equations

$$i\hbar \frac{d\langle B_{\mu}^{\dagger} \rangle}{dt} + \hbar \left(\omega_{\mu} + \frac{i}{T_{\mu}} \right) \langle B_{\mu}^{\dagger} \rangle - \mathbf{E}_{\text{opt}}(t) \cdot \mathbf{M}_{\mu}^{*} = \mathbf{E}_{\text{intra}}(t) \cdot \sum_{\mu'} \mathbf{G}_{\mu',\mu} \langle B_{\mu'}^{\dagger} \rangle \tag{8}$$

and

$$\begin{aligned} i\hbar \frac{d\langle B_{\mu}^{\dagger} B_{\nu} \rangle}{dt} = & -\hbar \left(\omega_{\mu} - \omega_{\nu} + \frac{i}{T_{\mu\nu}} \right) \langle B_{\mu}^{\dagger} B_{\nu} \rangle \\ & + \mathbf{E}_{\text{opt}}(t) \cdot [\mathbf{M}_{\mu}^{*} \langle B_{\nu} \rangle - \mathbf{M}_{\nu} \langle B_{\mu}^{\dagger} \rangle] \\ & + \mathbf{E}_{\text{intra}}(t) \cdot \sum_{\mu'} (\mathbf{G}_{\mu',\mu} \langle B_{\mu'}^{\dagger} B_{\nu} \rangle - \mathbf{G}_{\mu',\nu}^{*} \langle B_{\mu}^{\dagger} B_{\nu'} \rangle), \end{aligned} \tag{9}$$

where the self-induced intraband electric field is defined as

$$\mathbf{E}_{\text{intra}}(t) = -\frac{1}{\varepsilon_0 \varepsilon} \langle \mathbf{P}_{\text{intra}} \rangle. \tag{10}$$

Note that $\mathbf{E}_{\text{intra}}(t)$, in addition to containing an oscillating portion that generates the THz radiation coming from the Bloch-oscillating excitons, also contains a quasi-dc portion $\mathbf{E}_{\text{intra}}^{\text{dc}}$ arising from the permanent dipole moment of the excitons. It is this dc component that plays the critical role in the system dynamics considered in this paper. In Eq. (8), T_{μ} is the interband dephasing constant and is hereafter referred to as $T_{2\text{inter}}$. In Eq. (9), $T_{\mu\nu}$ is the intraband dephasing constant $T_{2\text{intra}}$ when $\mu \neq \nu$ and the exciton population lifetime $T_{1\text{ex}}$ when $\mu = \nu$. These time constants account phenomenologi-

cally for decoherence arising from such processes as carrier-carrier scattering, carrier-phonon scattering, and impurity scattering. In addition, the dephasing times account for any dephasing arising from inhomogeneous broadening due to spatial fluctuations in the superlattice potential.

In the derivation of Eqs. (8) and (9), in order to close the infinite hierarchy of equations, we have employed the factorizations

$$\langle B^{\dagger}_{\mu''} B_{\mu'''} B^{\dagger}_{\mu'} \rangle = \langle B^{\dagger}_{\mu''} B_{\mu'''} \rangle \langle B^{\dagger}_{\mu'} \rangle, \tag{11}$$

$$\langle B^{\dagger}_{\mu''} B_{\mu'''} B^{\dagger}_{\mu'} B_{\nu'} \rangle = \langle B^{\dagger}_{\mu''} B_{\mu'''} \rangle \langle B^{\dagger}_{\mu'} B_{\nu'} \rangle. \tag{12}$$

These equations generally follow the principle of a first-order cluster expansion[19] except that we have neglected the exciton-exciton exchange interaction. However, because we perform the first-order cluster expansion using an *exciton basis* rather than the usual *electron and hole basis*, the factorizations in Eqs. (11) and (12) make it possible for us to approximately include the second-order electron-hole Coulomb correlations, which are crucial in accounting for experimental phenomena such as dynamic screening.[28] Furthermore, employing the factorizations amounts to treating the dynamics nonperturbatively in the optical field and the self-generated internal intraband electric field $\mathbf{E}_{\text{intra}}$ is treated self-consistently. This allows the instantaneous net electric field to directly affect the exciton dynamics.

After solving the set of coupled nonlinear equations (8) and (9), we obtain the intraband polarization by taking the expectation value of Eq. (6). The emitted THz radiation signal is then calculated by taking the second derivative of this intraband polarization with respect to time. In the dynamics calculations, both $1s$-like excitonic states and higher-s-symmetry in-plane excitonic states[22] (HIES's) are included in the basis. The inclusion of HIES's is necessary to realistically and accurately account for experimental results, even in the low excitation limit.[22] Although, due to state mixing, the final excitonic eigenstates cannot be rigorously characterized as being, say, purely $1s$ or $2s$, for the convenience of discussion they can be approximately labeled by the pair of numbers $\mu=(n,m)$, where the index n gives approximately the nth WSL index as in the single-particle case and m gives the dominant quantum number for the in-plane radial motion of the exciton. In this scheme, the intraband dipole of the (n,m) state in the z direction is approximately $-ned$, where $n=\ldots,-2,-1,0,1,2,\ldots$, as is the case for single-particle WSL states. The states with $m=1$ are $1s$-like excitonic states, while the states with $m>1$ correspond to HIES's, up to continuum states.

III. SELF-GENERATED BLOCH OSCILLATIONS

A. Basic principles

Although in the usual experimental situation the coherences required for BO's are generated by an ultrashort optical pulse, there are alternative ways to achieve this. In this work, we are interested in producing coherences and hence BO's from the nonadiabatic change in the internal intraband electric field $\mathbf{E}_{\text{intra}}(t)$ in a BSSL. This intraband electric field is induced by the carriers generated by a spectrally narrow pulse. To simplify the discussion of how SBO's occur, let us for now consider only the $1s$ excitons. If the center frequency of the spectrally narrow pulse is in resonance with the $(-1,1)$ state, then to second order in the optical field, it cannot excite a superposition of excitonic WSL states in the dc field $\mathbf{F}_o$, but will only excite the $(-1,1)$ state ($|\chi_{-1}\rangle$). Now, for high optical intensities, as more excitons are created, the total dc field changes from $\mathbf{F}_o$ to $\mathbf{F}'=\mathbf{F}_o+\mathbf{E}^{\text{dc}}_{\text{intra}}$ due to the dipole moments of the generated excitons (see Sec. II). Thus, the excitons initially created in the field $\mathbf{F}_o$ are no longer eigenstates of the system with field $\mathbf{F}'$. If the field change from $\mathbf{F}_o$ to $\mathbf{F}'$ is adiabatic, then we still have no superposition state, as $|\chi_{-1}\rangle$ slowly (i.e., *adiabatically*) evolves into the eigenstate, $|\chi'_{-1}\rangle$, corresponding to the $(-1,1)$ state in the total field $\mathbf{F}'$. However, if the change is *nonadiabatic*, then we obtain a *superposition state* of $1s$ WSL eigenstates $|\chi'_p\rangle$ of the new field $\mathbf{F}'$. In the limit of an *instantaneous change* in the dc field at $t=0$ (i.e., the "sudden approximation"[45]), the state just after the field change will be $|\psi(t=0)\rangle=|\chi_{-1}\rangle$ so that $|\psi(t)\rangle=\Sigma_p\langle\chi'_p|\chi_{-1}\rangle e^{-ip\omega'_B t}|\chi'_p\rangle$ for $t\geqslant 0$. In general, if the field change is fast enough and large enough such that we are not in the adiabatic limit, then we expect to obtain a final state that is some sort of Bloch-oscillating superposition state, with the amplitude of the BO's determined to a large degree by the rate of change of the field.

The generation of Bloch-oscillating wave packets via a sudden change in the intraband field can also be described in terms of the spectral content of the intraband field. If we were to apply an external THz pulse to a photoexcited BSSL, then Bloch-oscillating wave packets may be generated due to the *THz-pulse-induced coherences* between the different WSL states, even if the exciting *optical pulse* is spectrally very narrow and thus generates no BO-related coherences by itself. In the picture of SBO's, the role of the external THz pulse is played by a nonadiabatic change in the internal dc electric field, the Fourier transform of which contains appreciable THz frequency components. If there are appreciable THz frequency components corresponding to the WSL spacing frequency ω_B, then intraband coherences will arise and we will obtain Bloch-oscillating excitonic wave packets.

B. Simple model for SBO's

Before considering the effects of exciton-exciton interactions on the self-induced internal intraband field and thus on SBO's in BSSL's, we first consider a simplified model where the dc electric field change is produced by a changing *external* dc field, rather than by the excitons themselves. We investigate a $GaAs/Ga_{0.7}Al_{0.3}As$ superlattice with a well width of 6.7 nm, barrier width of 1.7 nm, and external dc bias field of 11.5 kV/cm. All other parameters used in the calculation are given in Ref. 30. The linear absorption spectrum of the superlattice is shown in Fig. 1. In this work, we model the intraband dynamics and emitted THz radiation when the BSSL is excited either by a Gaussian pulse or a spectrally rectangular pulse (see Fig. 1). The intensity of the pulse is characterized by the peak areal excitonic density (per period) ρ generated by the pulse. The simulations are performed in-

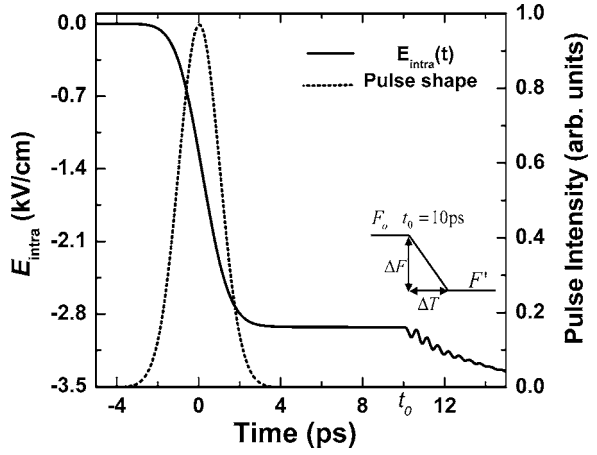

FIG. 2. The calculated intraband electric field as a function of time. Also shown is the temporal evolution of the intensity of the exciting Gaussian pulse and (schematically) the change in the bias field (inset). The simulation is done for a density of $\rho=0.95\times10^{10}$ cm^{-2}.

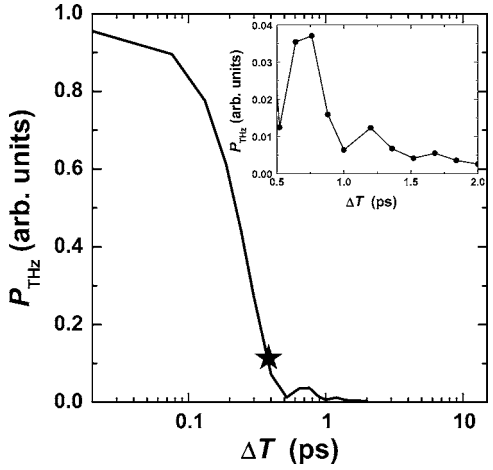

FIG. 3. Radiated THz emission power per exciton as a function of the time duration over which electric field change occurs for $\Delta F=-2$ kV/cm.

cluding HIES's up to 60 s and two-well basis states with an along-axis electron-hole separation ranging from $-8d$ to $8d$; with this basis, we obtain convergence in our results for the bias fields and carrier densities considered here.[28]

For convenience of discussion, in the simple model of this section, we take the exciton lifetime $T_{1\mathrm{ex}}$ to be infinite to clearly see how coherences are generated by a rapid field change. However, for the realistic calculations presented in the following sections, the exciton lifetime $T_{1\mathrm{ex}}$ is taken to be 2 ps. The exciton lifetime here refers to the time that an exciton remains in a particular excitonic eigenstate; it is not the recombination time for an exciton, which is much longer. The interband and intraband dephasing times are taken to be $T_{2\mathrm{inter}}=0.66$ ps and $T_{2\mathrm{intra}}=1.0$ ps, respectively, for all the simulations in this section. These are chosen to correspond approximately to those experimentally seen in recent experiments.[46] For these interband and intraband dephasing times we find that choosing a longer exciton lifetime (e.g., $\sim$10 ps) has very little effect on the results.

We now show how a rapid change in the bias field of the BSSL can generate BO's. We first populate primarily the $(-1,1)$ WSL state using a temporally long [temporal full width at half maximum (FWHM) of 2.77 ps] Gaussian pulse with a spectral FWHM of 0.19 THz (0.77 meV) centered on the $(-1,1)$ state (see Fig. 1). This pulse does not create populations in states such as $(-2,1)$ and (0,1) due to the narrow spectral width of the pulse; thus, no BO's are created for low intensities. Furthermore, as we shall show later, the duration of the pulse is sufficiently long that it does not generate a nonadiabatic change in the intraband field and thus will not result in SBO's, even for high intensities.

In Fig. 2, we plot the intraband field as a function of time for this system excited by the long Gaussian pulse. Because the $(-1,1)$ excitons each have a permanent dipole moment of approximately ed, a static intraband polarization—and hence internal intraband electric field—is generated when these excitons are created by the optical pulse. During the excitation process, as more and more polarized excitons are generated, the magnitude of this induced intraband quasi-dc field becomes larger and larger, until the pulse has passed. Then, starting at time $t_0=10$ ps, we linearly change the dc field applied to the BSSL by an amount of $-\Delta F$ over a time duration ΔT (see inset, Fig. 2). As soon as this field change begins, obvious oscillations (BO's) appear in the generated internal intraband electric field. These oscillations decay over a time of a few ps due to the finite intraband dephasing time constant $T_{2\mathrm{intra}}$. Thus, we see that the sudden change in the applied dc field results in the generation of Bloch-oscillating excitonic wave packets. We now investigate the THz power radiated from the oscillating excitonic wave packets as a function of the time duration and magnitude of the applied dc field change.

In Fig. 3, we present the calculated radiated THz power per exciton, P_{THz}, as a function of the time duration ΔT with ΔF fixed at -2 kV/cm. The radiated THz power is calculated by taking the square of second derivative of the intraband polarization and integrating over time; the emitted power per exciton is evaluated by dividing this power by the peak exciton density. As can be seen, the radiated THz power is strongly related to the time duration ΔT—i.e., the suddenness of the field change. In general, the smaller the ΔT, the larger the emitted THz power, with negligible THz power for $\Delta T\gtrsim0.5$ ps. However, the THz power P_{THz} becomes essentially saturated when the time duration ΔT falls below 0.02 ps. This is the time duration below which the *sudden approximation* becomes valid.[45] As we shall show, for the optical pulses considered in later sections, the time duration over which the *self-induced intraband field* changes lies between the adiabatic (very slow) and the sudden approximation—i.e., 0.02 ps$\lessapprox\Delta T\lessapprox$0.5 ps (Fig. 3). Thus for these excitations, at high enough intensities, a coherent Bloch-oscillating wave packet is self-generated.

In the inset to Fig. 3, we zoom in on the portion of the curve starting at $\Delta T=0.5$ ps. The small oscillations in the inset originate from the field-change function shown in the inset of Fig. 2. The discontinuity in the slope of the applied field generates multiple sidebands in its power spectrum. As ΔT increases, the sidebands in the power spectrum of the

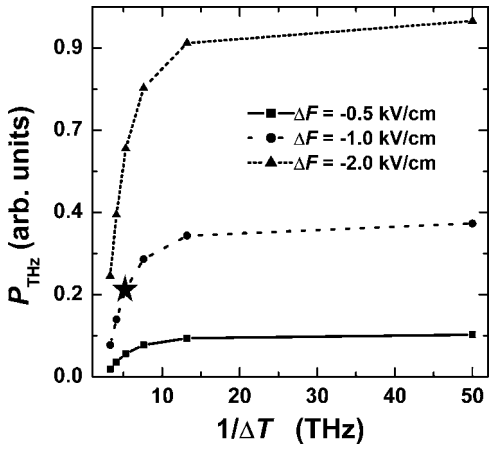

FIG. 4. Radiated THz power per exciton as a function of $1/\Delta T$ for different amplitudes ΔF of field change.

field-change function shift toward zero frequency. If for a specific ΔT two of the sidebands appear at $\omega = \pm \omega_B$, then WSL transitions are excited and the radiated THz power is a local maximum.[26]

Next we investigate the relation of the radiated THz power per exciton to the amplitude of the field change ΔF. To clearly show such a relation, we plot, in Fig. 4, P_{THz} versus $1/\Delta T$ for three different values of ΔF. For the range of ΔF considered, we see that the radiated THz power strongly depends on the amplitude of the field change within the BSSL. Returning to the intraband field change induced by the optical pulse (see Fig. 2), we note that for the approximately linearly varying portion from -0.3 to -2.3 kV/cm, ΔT is approximately 2.0 ps. Thus, referring to Fig. 3, we see that this optical pulse alone will not generate appreciable coherences, as is evidenced by the lack of oscillations near $t=0$ in the intraband field plotted in Fig. 2.

From the above discussions, we see that BO's can occur if a nonadiabatic field change is introduced in the BSSL. The power of the THz radiation from the SBO's is determined mainly by two factors: the suddenness of the field change, which is characterized by the time duration ΔT, and the amplitude of the field change ΔF. As expected, appreciable BO's are only generated if the time over which the field changes is less than or comparable to the inverse of the frequency separation, v_B, of the WSL levels—i.e., if $\Delta T \lessapprox \tau_B$ (Fig. 3), where τ_B is the Bloch oscillation period, which is around 0.42 ps for the BSSL considered here.

C. SBO's generated by spectrally narrow pulses

In Sec. III B, to clearly separate the contribution of the nonadiabatic field change to SBO's from other sources that may also generate coherences, we let the change in the dc field occur long after the optical pulse was gone (see Fig. 2). However, we have also found (not shown) that SBO's will occur in this same model if the field change happens while the Gaussian pulse is still present, which is closer to the actual physical situation that we will now examine.

We consider excitation with a spectrally rectangular pulse centered on the $(-1,1)$ excitonic state. Unlike in the simple model described in Sec. III B, here the dc field change is produced by the intraband field generated by the excitons themselves rather than by a simulated external one. The spectral width of the pulse is 1.5 THz (6.2 meV; see Fig. 1), which has been chosen such that it is narrower than the spacings between either the single particle or 1 *s* excitonic WSL states, which are approximately 10.4 meV (or 2.4 THz).

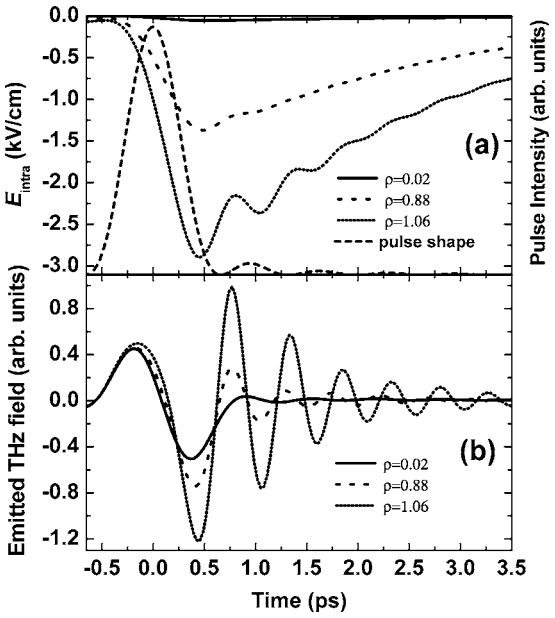

FIG. 5. (a) The calculated $E_{\mathrm{intra}}(t)$ for different densities. Also shown is the temporal evolution of the intensity of the exciting optical pulse. (b) The calculated, normalized, emitted THz fields (field per exciton) for the same densities as in (a). The densities are in units of 10^{10} cm^{-2}.

Figure 5(a) shows the unnormalized self-generated intraband electric field as a function of time for different exciton densities. For the lowest density, there are almost no oscillations in $E_{\mathrm{intra}}(t)$; the oscillations in the corresponding THz field shown in Fig. 5(b) arise entirely from the initial-dipole (ID) response, which is roughly the one-cycle THz oscilla-

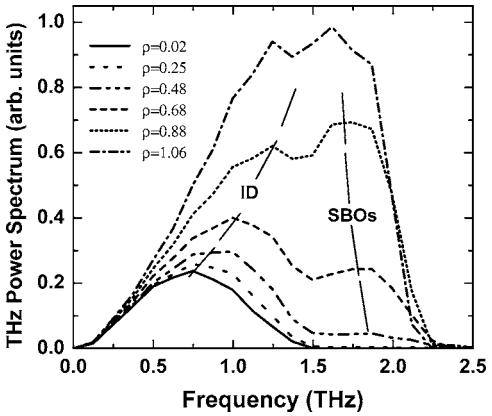

FIG. 6. The calculated THz spectra per exciton for different exciton densities for excitation via the spectrally rectangular pulse with a FWHM of 1.5 THz (6.2 meV) (see Fig. 1). The densities are in the units of 10^{10} cm^{-2}.

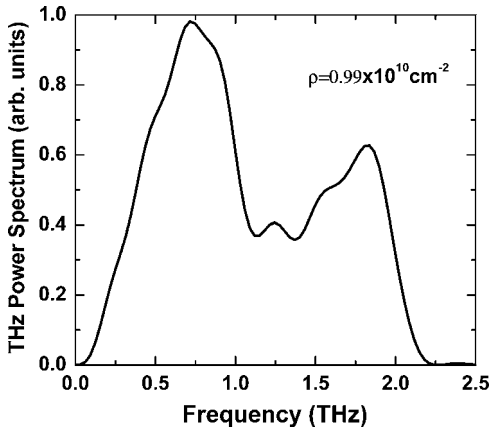

FIG. 7. The calculated THz spectra per exciton for excitation via the spectrally rectangular pulse with a FHWM of 1.06 THz (4.4 meV).

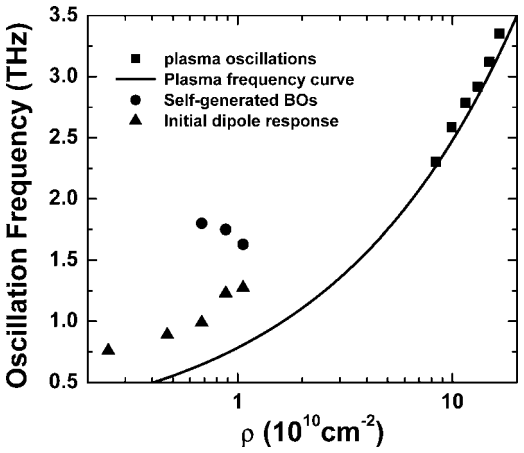

FIG. 8. The peak THz frequency as a function of exciton density for plasma oscillations, nonadiabatic BO's, and initial dipole response for excitation via the spectrally rectangular pulse with a FWHM of 1.5 THz (6.2 meV) (see Fig. 1). Also shown is the frequency versus density given by the expression from standard plasma theory [Eq. (13)].

tion associated with the sudden creation of excitons with permanent dipole moments.[47] The ID oscillations have a frequency of approximately 0.8 THz as can be seen in Fig. 6, where the power spectra of the emitted THz fields are plotted for a variety of densities.

As the density is increased, the peak frequency of the ID oscillation is *blueshifted* from 0.78 THz to 1.25 THz when the density changes from 0.02 to 0.88 (10^{10} cm^{-2}) (see Fig. 6). What is even more striking is that, as the density is increased, large oscillations in the intraband field also arise, which generates a substantial THz field long after the optical pulse is gone (see Fig. 5). These oscillations manifest themselves as a second peak in the THz power spectrum near 1.8 THz (see Fig. 6). Thus, a nonlinear optical response is being generated with a frequency much greater than the difference frequency between any of the spectral components of the exciting pulse. As we shall show, these oscillations are self-generated BO's. They are a clear signature of a nonlinear response well beyond second order in the optical field. Even for optical pulses that are more spectrally narrow (and hence longer in time), these SBO's can occur. In Fig. 7, we plot the THz spectrum arising from excitation with an spectrally rectangular optical pulse with a spectral width of 1.06 THz (4.4 meV; see Fig. 1) and an intensity such that the peak excitonic density is $\rho=0.99\times10^{10}$ cm^{-2}. As can be seen, there is a strong peak in the THz emission spectrum at 1.83 THz for this excitonic density.

As discussed in the simple model of Sec. III B, the THz power per exciton arising from SBO's depends strongly on two main factors: the suddenness and amplitude of the internal intraband field change. This is also true in the physically realistic simulations considered here. As the density is increased, the amplitude of the field change is also increased [Fig. 5(a)] and the THz power per exciton increases (Fig. 6).

Regarding the *suddenness* of the field change, the situation with realistic excitation is more complicated than the simulated quasistep function shown in the inset to Fig. 2. As shown in Fig. 5(a), the slope of E_{intra} changes continuously during the excitation process. To allow comparison to the results of Sec. III B, we first consider the time duration over which the field changes from -1 kV/cm to -2 kV/cm for the case of $\rho=1.06\times10^{10}$ cm^{-2}; this time duration is just 0.19 ps as shown in Fig. 5(a). Comparing this to the case of $\Delta F=-1$ kV/cm in Fig. 4 at $1/\Delta T=1/0.19$ ps$\simeq$5.26 THz (marked by a star), we see that the field indeed varies nonadiabatically and thus should produce appreciable THz emission power, as shown in Fig. 5(b). Now, even if we consider the time over which the field changes by -2 kV/cm from -0.5 to -2.5 kV/cm, the time duration is still only 0.38 ps. Thus, referring to Fig. 3 (marked by star) we see that this rate of change also falls within the nonadiabatic change range. Thus, it is clear from both these comparisons that we would expect to see SBO's due to the nonadiabatic field change for this density, but that we are far from the sudden approximation.

For moderate to high excitations, the suddenness of the field change is enhanced due to the blue shifting of the $n<0$ WSL states with time.[28] As the dc field builds up, the WSL energies are renormalized, as can be seen in the redshift in the SBO frequency with increasing density (see Fig. 6). Thus, while only $(-1,1)$ excitons are created near the beginning of the pulse, towards the end of the pulse, largely $(-2,1)$ excitons are created since they are now in resonance with the pulse spectrum. Thus the total intraband electric field changes more quickly than it would if only $(-1,1)$ excitons were created. Therefore, the change in the intraband electric field becomes steeper and the ID-generated THz emission blueshifts as the density increases (Fig. 6). This can be seen in Fig. 5(b) where the normalized THz emission corresponding to the highest density completes its first oscillation cycle much earlier than the ones with lower densities. This indicates that the E_{intra} corresponding to the highest excitation approaches its maximum faster than the ones with the lower excitations. This density-dependent self-steepening process helps to increase the suddenness of field change and thus considerably enhances the THz power emitted due to SBO's.

D. Comparison to plasma oscillations

In previous work,[28] we have shown that at very high densities ($\rho \gtrsim 10^{11}$ cm^{-2}), BO's evolve into PO's due to *dynamic* screening. To confirm that the SBO's being investigated are indeed BO's and not PO's, we use the data from the calculated spectra to plot in Fig. 8 the density-dependent peak THz frequency for plasma oscillations, SBO's, and initial dipole response. To fit the numerically calculated plasma frequency, we also plot a plasma frequency curve using the usual density-dependent plasma expression[48]

$$\omega_{pl} = \sqrt{\frac{e^2 n_0}{\epsilon_0 \epsilon_b m_{pl}^*}}, \tag{13}$$

where $n_0 = \rho d$ is the volume density and m_{pl}^* is the reduced effective plasma mass for the electron-hole pairs. Taking the plasma mass to be a fitting parameter, we find that we obtain an excellent fit to the nonperturbative results using Eq. (13) with a plasma mass of $m_{pl}^* = 0.125 m_0$, where m_0 is the free electron mass.[49]

As discussed in the previous section, due to the increasing self-induced dc field within the superlattice, we see that the SBO peak redshifts with increasing density from 1.82 THz to 1.64 THz at the highest density; this is in direct contrast to the blueshift expected for PO's. When extrapolating the frequency of PO's to low exciton densities from the plasma frequency curve obtained by Eq. (13), we find that the frequencies of SBO's are much larger than those of PO's at the corresponding densities. Moreover, the normalized amplitude of the SBO's goes up as density goes up (Fig. 6), while the normalized amplitude of PO's always goes down as density goes up (not shown). It is therefore clear that the oscillations that we have identified as SBO are not PO's and can only be attributed to SBO's.

IV. CONCLUSIONS

We have calculated the highly nonlinear ultrafast intraband response of a BSSL. In particular, we have demonstrated a new and surprising mechanism for the generation of BO's based on the nonadiabatic change of the self-induced internal dc field in the BSSL. By examining the effects of a rapid change in the internal bias field of a BSSL and via direct simulation, we clearly demonstrate the origin of these oscillations and show that they can be clearly distinguished from plasma oscillations. Given that the changes in the intraband fields described in this work have been experimentally seen for Gaussian-pulse excitation,[28] we are confident that further ultrafast experiments can and should be done on this system to demonstrate this exciting new nonlinear effect.

The system dynamics were modeled employing an exciton formalism. In order to simplify the calculations, we neglected so-called phase-space filling effects[24,28] that arise from the deviation of excitons from perfect bosons. However, for the densities at which the SBO's appear, it is easy to show that such effects will be quite weak.[27] However, in future work we hope to include such effects, along with microscopic scattering mechanisms.

ACKNOWLEDGMENTS

The authors thank Ben Rosam and Karl Leo for fruitful discussions. This work was supported in part by the Natural Sciences and Engineering Research Council of Canada.

[1] C. Zener, Proc. R. Soc. London, Ser. A **145**, 523 (1934).
[2] F. Bloch, Z. Phys. **52**, 555 (1928).
[3] Hubert M. James, Phys. Rev. **76**, 1611 (1949).
[4] G. H. Wannier, *Elements of Solid State Theory* (Cambridge University Press, Cambridge, England, 1959), p. 190.
[5] G. H. Wannier, Phys. Rev. **117**, 432 (1969).
[6] E. E. Mendez, F. Agulló-Rueda, and J. M. Hong, Phys. Rev. Lett. **60**, 2426 (1988).
[7] P. Voisin, J. Bleuse, C. Bouche, S. Gaillard, C. Alibert, and A. Regreny, Phys. Rev. Lett. **61**, 1639 (1988).
[8] L. Esaki and R. Tsu, IBM J. Res. Dev. **14**, 61 (1970).
[9] J. Shah, *Ultrafast Spectroscopy of Semiconductors and Semiconductor Nanostructures*, 2nd enlarged ed. (Springer, Berlin 1999).
[10] G. von Plessen and P. Thomas, Phys. Rev. B **45**, 9185 (1992).
[11] J. Feldmann, K. Leo, J. Shah, D. A. B. Miller, J. E. Cunningham, T. Meier, G. von Plessen, A. Schulze, P. Thomas, and S. Schmitt-Rink, Phys. Rev. B **46**, R7252 (1992).
[12] K. Leo, P. Haring Bolivar, F. Brüggemann, R. Schwedler, and K. Köhler, Solid State Commun. **84**, 943 (1992).
[13] P. Leisching, P. Haring Bolivar, W. Beck, Y. Dhaibi, F. Brüggemann, R. Schwedler, H. Kurz, K. Leo, and K. Köhler, Phys. Rev. B **50**, 14389 (1994).
[14] C. Waschke, H. G. Roskos, R. Schwedler, K. Leo, H. Kurz, and K. Köhler, Phys. Rev. Lett. **70**, 3319 (1993).
[15] H. Roskos, C. Waschke, R. Schwedler, P. Leisching, Y. Dhaibi, H. Kurz, and K. Köhler, Superlattices Microstruct. **15**, 281 (1994).
[16] C. Waschke, P. Leisching, P. H. Bolivar, R. Schwedler, F. Brüggemann, H. G. Roscos, K. Leo, H. Kurz, and K. Köhler, Solid-State Electron. **37**, 1321 (1994).
[17] V. M. Axt and S. Mukamel, Rev. Mod. Phys. **70**, 145 (1998).
[18] V. M. Axt, G. Bartels, and A. Stahl, Phys. Rev. Lett. **76**, 2543 (1996).
[19] F. Rossi and T. Kuhn, Rev. Mod. Phys. **74**, 895 (2002).
[20] J. Hader, T. Meier, S. W. Koch, F. Rossi, and N. Linder, Phys. Rev. B **55**, 13799 (1997).
[21] F. Löser, M. M. Dignam, Yu. A. Kosevich, K. Köhler, and K. Leo, Phys. Rev. Lett. **85**, 4763 (2000).
[22] L. Yang, B. Rosam, J. M. Lachaine, K. Leo, and M. M. Dignam, Phys. Rev. B **69**, 165310 (2004).
[23] J. M. Lachaine, Margaret Hawton, J. E. Sipe, and M. M. Dignam, Phys. Rev. B **62**, R4829 (2000).
[24] M. M. Dignam and M. Hawton, Phys. Rev. B **67**, 035329 (2003).
[25] T. Meier, G. von Plessen, P. Thomas, and S. W. Koch, Phys. Rev. Lett. **73**, 902 (1994).
[26] B. Rosam, L. Yang, K. Leo, and M. M. Dignam, Appl. Phys. Lett. **85**, 4612 (2004).
[27] M. Hawton and M. M. Dignam, Phys. Rev. Lett. **91**, 267402 (2003).

[28] L. Yang, B. Rosam, and M. M. Dignam, Phys. Rev. B **72**, 115313 (2005).
[29] J. Zak, Phys. Rev. Lett. **20**, 1477 (1968).
[30] M. M. Dignam and J. E. Sipe, Phys. Rev. Lett. **64**, 1797 (1990); Phys. Rev. B **43**, 4097 (1991).
[31] H. Haug and S. W. Koch, *Quantum Theory of the Optical and Electronic Properties of Semiconductors*, 3rd ed. (World Scientific, Singapore, 1994).
[32] S. Glutsch and F. Bechstedt, Phys. Rev. B **60**, 16584 (1999).
[33] N. Linder, Phys. Rev. B **55**, 13664 (1997).
[34] M. Dignam, J. E. Sipe, and J. Shah, Phys. Rev. B **49**, 10502 (1994).
[35] H. Haug, *Ultrafast Physical Progresses in Semiconductors*, edited by K. T. Tsen, Semiconductors and Semimetals, No. 67 (Academic, San Diego, 2001).
[36] D. S. Chemla and J. Shah, Nature (London) **411**, 549 (2001).
[37] V. G. Lyssenko, G. Valusis, F. Löser, T. Hasche, K. Leo, M. M. Dignam, and K. Köhler, Phys. Rev. Lett. **79**, 301 (1997).
[38] H. Haug and A.-P. Jauho, *Quantum Kinetics in Transport and Optics of Semiconductors* (Springer, Berlin, 1996).
[39] G. Bartels, G. C. Cho, T. Dekorsy, H. Kurz, A. Stahl, and K. Köhler, Phys. Rev. B **55**, 16404 (1997).
[40] Th. Östreich, K. Schönhammer, and L. J. Sham, Phys. Rev. B **58**, 12920 (1998).
[41] C. Sieh, T. Meier, F. Jahnke, A. Knorr, S. W. Koch, P. Brick, M. Hübner, C. Ell, J. Prineas, G. Khitrova, and H. M. Gibbs, Phys. Rev. Lett. **82**, 3112 (1999); C. Sieh, T. Meier, A. Knorr, F. Jahnke, P. Thomas, and S. W. Koch, Eur. Phys. J. B **11**, 407 (1999).
[42] T. Meier, S. W. Koch, P. Brick, C. Ell, G. Khitrova, and H. M. Gibbs, Phys. Rev. B **62**, 4218 (2000).
[43] O. E. Raichev, F. T. Vasko, A. Hernández-Cabrera, and P. Aceituno, Phys. Rev. B **56**, 4802 (1997).
[44] L. J. Sham and T. M. Rice, Phys. Rev. **144**, 708 (1966).
[45] A. Messiah, *Quantum Mechanics* (John Wiley and Sons, New York, 1961), Chap. XVII.
[46] P. H. Bolivar, F. Wolter, A. Muller, H. G. Roskos, H. Kurz, and K. Köhler, Phys. Rev. Lett. **78**, 2232 (1997).
[47] Paul C. M. Planken, Igal Brener, Martin C. Nuss, M. S. C. Luo, S. L. Chuang, and L. N. Pfeiffer, Phys. Rev. B **49**, 4668 (1994).
[48] N. W. Ashcroft and N. D. Mermin, *Solid State Physics* (Holt, Rinehart, and Winston, Philadelphia, 1976).
[49] This is the same mass that was used to model the plasma oscillations in Ref. 28 under somewhat different excitation conditions.